Neuron, Vol. 39, 589–598, August 14, 2003, Copyright ©2003 by Cell Press

Structure of the Semaphorin-3A Receptor Binding Module

Report

Alexander Antipenko,[1] Juha-Pekka Himanen,[1] Klaus van Leyen,[1,5] Vincenzo Nardi-Dei,[1,6] Jacob Lesniak,[1] William A. Barton,[1] Kanagalaghatta R. Rajashankar,[2] Min Lu,[3] Claudia Hoemme,[4] Andreas W. Püschel,[4] and Dimitar B. Nikolov[1,*]

[1]Cellular Biochemistry and Biophysics Program
Memorial Sloan-Kettering Cancer Center
1275 York Avenue
New York, New York 10021
[2]Brookhaven National Laboratory
Brookhaven, New York 11973
[3]Department of Biochemistry
Weill Medical College of Cornell University
New York, New York 10021
[4]Abt. Molekularbiologie
Institut für Allgemeine Zoologie und Genetik
Westfälische Wilhelms-Universität
D-48149 Münster
Germany

Summary

The semaphorins are a large group of extracellular proteins involved in a variety of processes during development, including neuronal migration and axon guidance. Their distinctive feature is a conserved 500 amino acid semaphorin domain, a ligand-receptor interaction module also present in plexins and scatter-factor receptors. We report the crystal structure of a secreted 65 kDa form of Semaphorin-3A (Sema3A), containing the full semaphorin domain. Unexpectedly, the semaphorin fold is a variation of the β propeller topology. Analysis of the Sema3A structure and structure-based mutagenesis data identify the neuropilin binding site and suggest a potential plexin interaction site. Based on the structure, we present a model for the initiation of semaphorin signaling and discuss potential similarities with the signaling mechanisms of other β propeller cell surface receptors, such as integrins and the LDL receptor.

Introduction

The semaphorins are axon guidance signals that are defined by the presence of a conserved 500 amino acid semaphorin domain at their amino termini, which serves as a receptor recognition and binding module (reviewed in Fiore and Püschel, 2003). Semaphorin 3A (Sema3A) was the first molecularly characterized chemorepellent and acts via a receptor complex that contains Neuropilin 1 (Nrp-1) as the ligand binding subunit and an A-Plexin as the signal-transducing subunit (Fiore and Püschel, 2003) (Figure 1A). Nrp-1 and the closely related Nrp-2 appear to bind all class 3 semaphorins but differ in their affinity for individual members (Fiore and Püschel, 2003; He and Tessier-Lavigne, 1997; Kolodkin et al., 1997). Nrp-1 is an integral membrane protein with a large extracellular domain, a single transmembrane domain, and a short cytoplasmic tail. The neuropilin extracellular domain contains two CUB motifs (domain A: A1, A2), followed by two domains with similarity to coagulation factor V/VIII (domain B: B1, B2) and one MAM domain (domain C). Both domains A and B are essential for binding the semaphorin domain of Sema3A, while only B1 is required for the interaction with VEGF165 or the basic carboxy terminus of Sema3A (Giger et al., 1998; Gu et al., 2002; Lee et al., 2003; Nakamura et al., 1998; Renzi et al., 1999). While the C terminus does not contribute to the biological specificity of semaphorins, it is a major determinant of their affinity for neuropilins (Giger et al., 1998; Nakamura et al., 1998).

Vertebrate A-Plexins are the signaling subunits for secreted class 3 semaphorins, while other plexins interact with semaphorins of different classes (Fiore and Püschel, 2003). In contrast to Sema3A, which is not able to bind directly to A-Plexins, Sema4D and Sema7A directly interact with Plexin-B1 and Plexin-C1, respectively (Takahashi et al., 1999; Tamagnone et al., 1999). Interestingly, all plexins contain an extracellular semaphorin domain that is strictly required for their function (Figure 1A). A semaphorin domain is also present in the scatter-factor receptor MET (Tamagnone et al., 1999). In order to gain an insight into the molecular mechanisms of semaphorin-mediated signaling, we have determined the structure of a functional 65 kDa Sema3A form (Sema3A-65K) containing the full semaphorin domain and propose a mechanism for initiation of Sema3A-mediated signaling.

Results and Discussion

Functional Characterization of Recombinant Sema3A-65K

Sema3A-65K (residues 26–546; Figure 1A) was expressed as a soluble secreted protein in insect cells using the baculovirus system. Sema3A-65K specifically bound Nrp1-AB (containing domains A1, A2, B1, and B2) with submicromolar (230 nM) affinity while interacting only weakly with Nrp1-A (A1 + A2) or Nrp1-B (B1 + B2), as shown by tryptophane fluorescence titration spectroscopy (Figure 1B). Its biological activity was shown in a heterologous system that mimics growth cone collapse (Takahashi et al., 1999; Zanata et al., 2002). Sema3A-65K induced the collapse of transfected COS-7 cells that become responsive to Sema3A upon coexpression of Plexin-A1 and Nrp-1 with an EC_{50} of 1.9 μM (Figures 1C and 1D). The difference in the biological activities of Sema3A-65K and of full-length Sema3A (EC_{50} of 0.1 nM) is partially due to the fact that semaphorin dimerization is required for eliciting full response

*Correspondence: dimitar@ximpact3.ski.mskcc.org
[5]Present address: Massachusetts General Hospital, Charlestown, Massachusetts 02129.
[6]Present address: Chiron Research Center, 53100 Siena, Italy.

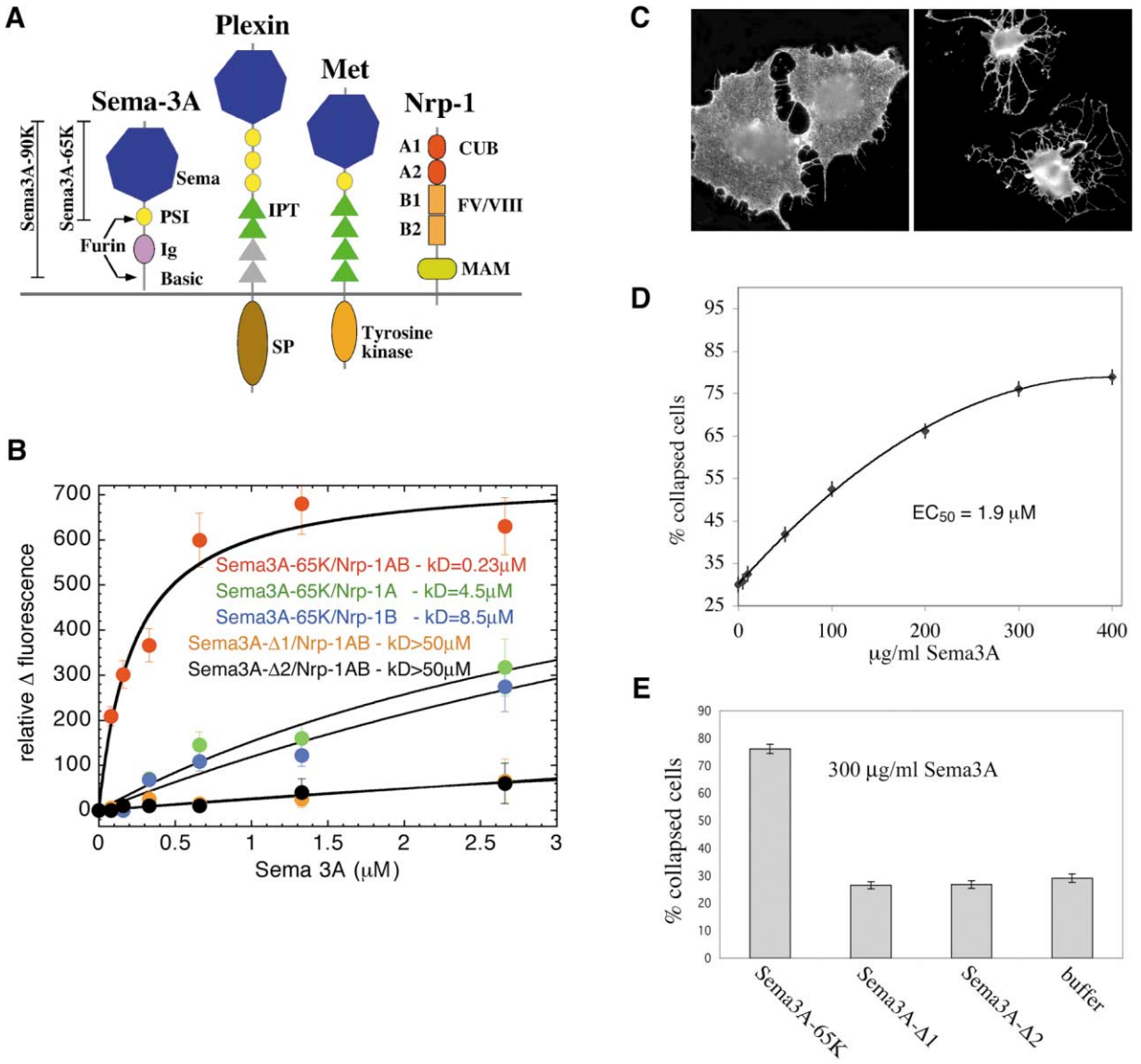

Figure 1. Biological Activity of Sema3A-65K

(A) Schematic representation of the domain organization of semaphorins, neuropilins, plexins, and scatter-factor receptors. The individual domains are labeled. PSI, Plexin/Semaphorin/Integrin domain; IPT, Immunoglobulin-like domain found in Plexins (and Met) and in some Transcription factors; CUB, domain homologous to complement binding factors C1r and C1s; FV/VIII, domain homologous to coagulation factor V and VIII (also known as F5/8 type C or discoidin domain); MAM, Mephrin/A5/μ domain; SP, Sex-Plexin domain. The arrows indicate the locations of the furin processing sites in Sema3A (Adams et al., 1997). Semaphorins, plexins, and scatter-factor receptors share a common semaphorin domain (blue heptagon).

(B) Binding of recombinant Sema3A-65K, Sema3A-Δ1, and Sema3A-Δ2 to recombinant Nrp-1 measured by fluorescence titration spectroscopy. Data points represent means of multiple measurements, and the bars represent standard errors. The curves are unweighted least-squares fits to a standard dissociation equilibrium equation.

(C) Sema3A-65K induces cytoskeletal collapse in cells expressing Plexin-A1 and Nrp-1. COS-7 cells were transfected with expression vectors for VSV-PlexinA1 and HA-Nrp-1 and incubated with buffer (left) or increasing amounts of Sema3A-65K (right) for 1 hr at 37°C.

(D) The estimated EC_{50} for Sema3A-65K is 1.9 μM. Cells were fixed, processed for indirect immunofluorescence using an anti-VSV antibody, and the number of collapsed cells determined.

(E) Sema3A-Δ1 and Sema3A-Δ2 do not induce cytoskeletal collapse in the same assay. The concentration of recombinant semaphorin was 300 μg/ml.

(Klostermann et al., 1998; Koppel and Raper, 1998). While full-length Sema3A (Sema3A-90K) is dimerized prior to receptor binding via a disulfide bridge, Sema3A-65K is not a covalent dimer. In addition, the basic C-terminal semaphorin tail, while not directly contributing to receptor specificity, increases the affinity of the molecule for its membrane bound receptors (He and Tessier-Lavigne, 1997; Feiner et al., 1997).

Structure of Sema3A-65K

The structure of Sema3A-65K was determined using two-wavelength MAD phasing (see the Supplemental

Data available online at http://www.neuron.org/cgi/content/full/39/4/589/DC1) with data collected from a crystal produced with seleno-methionine-modified protein. The final model is refined at 2.8 Å resolution to an R factor of 24.9% (free R of 29.4%). Sema3A-65K (Figures 2A, 3A, and 3B) is an elongated disc-shaped molecule with approximate dimensions of 60 × 70 × 45 Å. Unexpectedly, the semaphorin fold is a variation of the β propeller topology (Paoli, 2001; Fulop and Jones, 1999), with seven blades radially arranged around a central axis. Each blade contains a four-stranded (strands A to D) antiparallel β sheet. The inner strand of each blade (A) lines the channel at the center of the propeller, with strands B and C of the same repeat radiating outward, and strand D of the next repeat forming the outer edge of the blade (Figure 3). In contrast to most known β propeller structures with approximately 40–45 residues per blade, the semaphorin blades average 70 amino acids (Figure 3E). The large size of the semaphorin domain is not due to a single inserted domain but results from the presence of additional secondary structure elements inserted in most of the blades. Specifically, semaphorin blade 1 contains an additional strand (1S1) and a helix (1H1), blade 2 has two inserted helices (2H1 and 2H2), blade 4 has an extra helix (4H1), and blade 5 has the largest insertion composed of three helices (5H1, 5H2, and 5H3) and two β strands (5S5 and 5S6). Some of the loops connecting the secondary structure elements are also unusually long (see Figure 3B), including the four loops that form the proposed neuropilin binding site (Figures 2A and 4D).

The individual propeller β strands are in extended conformation, with radially directed hydrogen bonds. These mainchain hydrogen bonds are accessible at the surface of the propeller and could potentially mediate interactions with other proteins. The central tunnel is not cylindrical but is slightly conical in shape with the end defined by the N-terminal parts of the A strands (at the "top face" of the molecule) narrower than the C-terminal side (at the "bottom face").

Like most of the other known propeller structures, semaphorin uses a "loop and hook" system to close the circle between the first and the last blades (Paoli, 2001; Fulop and Jones, 1999). The Sema's loop and hook (Figure 3) are stronger than usually observed. Indeed, the N terminus of the molecule, in addition to contributing the fourth (D) antiparallel β strand of the seventh blade (purple), wraps further around and contributes a fifth, this time parallel, strand to the sixth blade (blue). Four disulfide bonds also stabilize the structure: Cys 103 – Cys 114, Cys 132 – Cys 144, Cys 269 – Cys 381, and Cys 293 – Cys 341. Two of these are within the second blade and two connect the fourth and the fifth blades. The fourth and fifth blades contain more elaborate structural features, including long protruding loops that form the proposed neuropilin interaction site (see Discussion further below). Semaphorin is a glycosylated protein, and N-linked N-acetyl-β-D-glucosamine moieties, modifying Asn-53 and Asn-125, were clearly identifiable in the electron density map and were built into the model.

On the basis of sequence homology, the semaphorin residues 515–568 are predicted to fold into a so-called PSI domain (Bork et al., 1999) (Figure 1A). Part of this sequence is present in Sema3A-65K (the furin processing site is at position 546) and is partially ordered, but the electron density in the region is weak, and it cannot be built into the semaphorin model. PSI domains are present in other extracellular proteins, but their structures are not known. In integrin β3, the structure of which was recently reported (Xiong et al., 2001), the PSI domain was also not well ordered in the crystals.

Structural Homology to Other Proteins

A comparison of the Sema3A structure with the contents of the FSSP database (Holm and Sander, 1998) reveals structural similarity with other β propeller-containing proteins. The closest structural homologs of Sema3A are the β subunit of the trimeric G protein transducin (Sondek et al., 1996), the transcriptional repressor tup1 (Sprague et al., 2000), Arp3 (Robinson, et al., 2001), and integrin αV (Xiong et al., 2001). The seven-bladed β propeller domains of these proteins can be superimposed on the corresponding regions of Sema3A with root-mean-square deviations (rms) between α carbon positions of 3.3 Å for transducin (for a selected 282 atoms), 3.3 Å for tup1 (287 atoms), 3.7 Å for Arp3 (282 atoms), and 4.1 Å for integrin (302 atoms). The semaphorin β propeller structure is bigger than its structural homologs (Figure 3A), and only the regions containing the four innermost strands (A, B, C, and D) of the semaphorin blades can be superimposed, since only they have direct structural counterparts.

Semaphorins, plexins, and scatter-factor receptors were not recognized until now as β propeller proteins, because they lack any detectable repeating motifs in their sequences. Even in light of the Sema3A structure, a superposition of the seven semaphorin blades fails to reveal any consensus sequence repeat (Figure 3E). In contrast, most other β propellers are stabilized by different sets of interactions that result in sequence repeats (or motifs) shared by all or most individual modules. For example, in the WD repeats of Gβ, the residues Trp-Ser/Thr-His-Asp form an electrostatic tetrad reoccurring throughout the circular array. Other such motifs include the YWTD, TolB, RCC1, and Tachylectin-2 repeats, the aspartate box, and the (WD), *kelch* and tryptophan-docking motifs (Fulop and Jones, 1999). Instead of repeating sequence or structural motifs, the semaphorin fold is partially stabilized by the conserved disulfide bonds, which contribute to maintaining the protein architecture while allowing divergence in the sequence. In this respect, semaphorin is similar to viral neuraminidase, the six-bladed propeller of which has 9 disulfide bonds and very little interrepeat sequence similarity (Varghese et al., 1983; Paoli, 2001).

Sema3A-65K Dimerization and Stoichiometry of the Sema3A-65K/Nrp-1AB Complex

Sema3A-65K migrates as a dimer during gel filtration and is a dimer in the crystals (Figure 2A). The two monomers in the asymmetric unit are structurally very similar (rmsd for equivalent Cα positions is 0.45 Å), except for the crystallographic packing at two flexible surface loops. The monomers bind each other using four protruding surface loops, 4S3-4S4 (*B4-C4*), 5S1-5S2 (*D4-A5*), 5S3-5S4 (*B5-C5*), and 5S5-5S6 (*C5-D5*), which intertwine with each other to form an intimate and extensive interface burying a total of 2900 Å^2 (1450 Å^2 in each

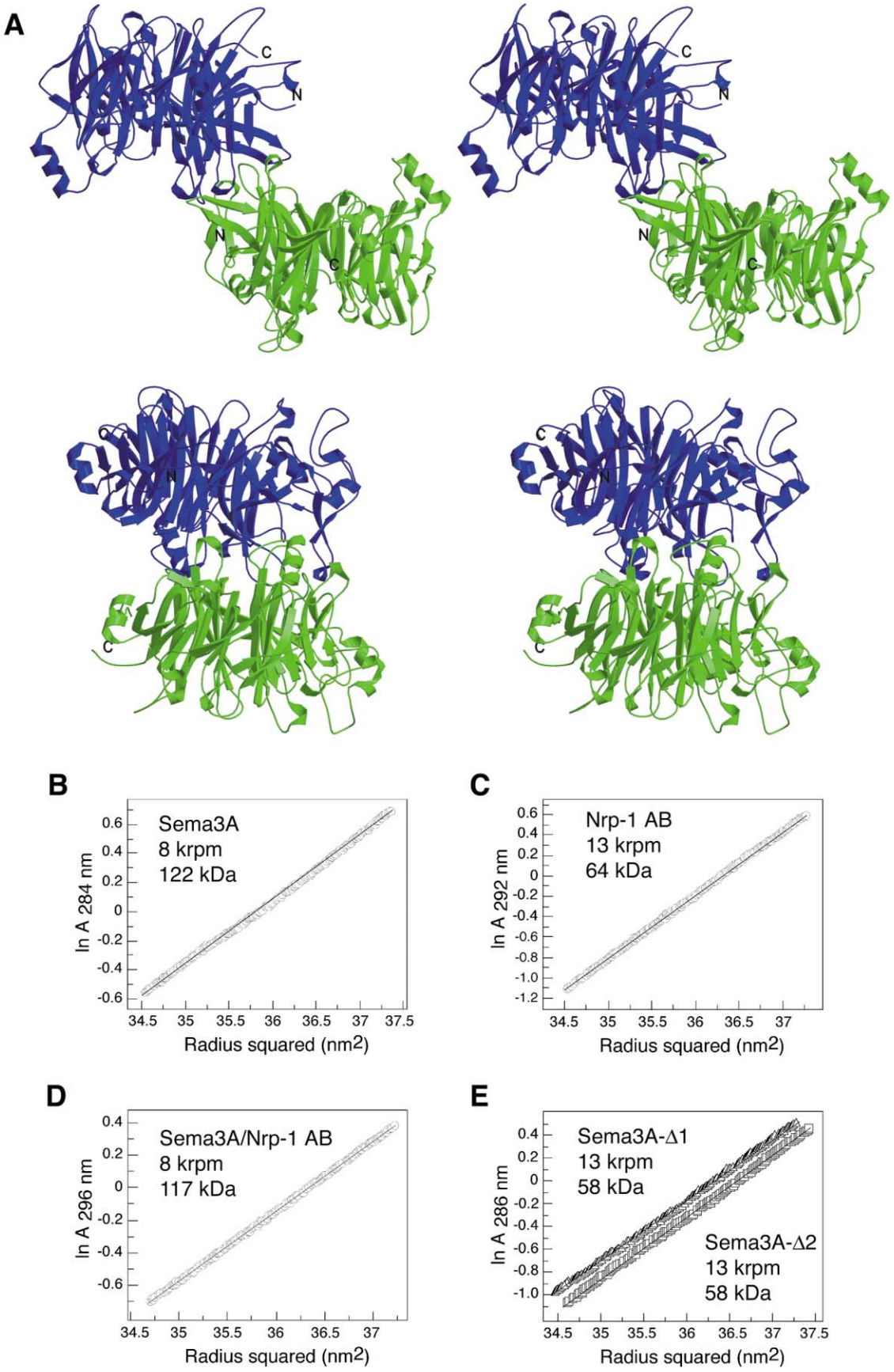
A
C
N
N
C
C
N
N
C
C
N
N
C
C
N
N
C
B
Sema3A
8 krpm
122 kDa
ln A 284 nm
Radius squared (nm2)
C
Nrp-1 AB
13 krpm
64 kDa
ln A 292 nm
Radius squared (nm2)
D
Sema3A/Nrp-1 AB
8 krpm
117 kDa
ln A 296 nm
Radius squared (nm2)
E
Sema3A-Δ1
13 krpm
58 kDa
Sema3A-Δ2
13 krpm
58 kDa
ln A 286 nm
Radius squared (nm2)

monomer). The interface contains both hydrophobic (~40% of the total) and polar residues, and the molecular interactions between them include hydrogen bonds, salt bridges, and Van der Waals contacts. We further investigated the oligomeric states of the protein and of its receptor Nrp-1AB in solution, as well as the stoichiometry of their interaction using analytical ultracentrifugation. The experiments summarized in Figures 2B–2D document that Sema3A-65K is a dimer in solution (the estimated Kd of dimerization is 3 μM; data not shown) and undergoes a dimer-to-monomer transition upon binding to monomeric Nrp-1AB (Kd of 0.23 μM; Figure 1B), thus forming a 1:1 complex. The neuropilin complex formed by Sema3A-90K (or "full-length" Sema3A), which is the predominant Sema3A form in vivo (Adams et al., 1997), is expected to have a 2:2 stoichiometry, since Sema3A-90K is a preformed covalent dimer via a disulfide bridge located outside of the receptor binding domain (see Figure 5A).

The Neuropilin Binding Site

The fact that neuropilin binding competes with semaphorin dimer formation indicates that the neuropilin binding region of Sema3A overlaps with or is very close to the dimerization interface. Our data further suggests that the neuropilin binding surface of the semaphorins is likely localized to the upper part of the top face of the β propeller, centered around the protruding flexible loops of blades 4 and 5 (blue and green on Figure 3A). Since all class 3 semaphorins bind neuropilins, while class 4 semaphorins do not (Fiore and Püschel, 2003), a structure-based analysis of the conservation of semaphorin residues should yield insight into the location of important ligand/receptor interfaces. Figure 4A shows in cyan all surface-exposed residues, which are conserved only within class 3 molecules but not between the 3 and 4 classes (see also the Supplemental Data at http://www.neuron.org/cgi/content/full/39/4/589/DC1). The only substantial continuous surface patch with this conservation profile (blue circle in Figure 4A) overlaps with the Sema3A-65K dimerization interface (Figure 4C). Furthermore, analysis of the electrostatic potential on the molecular surface of Sema3A reveals that the top face of the molecule (Figure 4B, left) is positively charged, particularly around blades 3 and 4, while the bottom face contains many acidic surface-exposed residues (Figure 4B, right). Neuropilin-1 is negatively charged with a pI value of 5.5 for both the whole extracellular and the Nrp-1AB regions and is thus likely to interact with the basic Sema3A region.

To understand better the role of the surface loops that mediate Sema3A-65K dimerization (magenta on Figure 4C), in Nrp-1 binding, we engineered two Sema3A-65K variants, containing a deletion of the 4S3-4S4 (*B4-C4*) loop (Sema3A-Δ1: deletion of residues 252–260, green in Figure 4D) or the 5S5-5S6 (*C5-D5*) loop (Sema3A-Δ2: residues 359–366, orange in Figure 4D). Sema3A-Δ1 and Sema3A-Δ2 are properly folded, as judged by CD spectroscopy (data not shown), but are monomeric even at millimolar concentrations both during gel filtration chromatography and in analytical ultracentrifugation experiments (Figure 2E). Importantly, both Sema3A mutants do not bind Nrp-1 (Figure 1B) and do not promote cytoskeletal collapse (Figure 1E). These results confirm that the high-affinity semaphorin-neuropilin interface indeed falls within the area circled on Figure 4A. Interestingly, a Sema3A-neutralizing antibody was previously shown to target specifically the loop deleted in Sema3A-Δ2 (Shirvan et al., 2002). Peptides corresponding to Sema3A residues 363–380 (5S5-5H2/*C5-D5*, Figure 3E) mimick the biological activity of full-length Sema3A (Shirvan et al., 2002). Finally, the closest structural homologs of Sema3A, namely, the transducin β subunit and integrin, utilize corresponding surfaces on their β propellers to bind their respective interaction partners (Xiong et al., 2001; Sondek et al., 1996). Specifically, the interaction interfaces are located on the top face of the propeller, slightly off-center, with most interface residues belonging to blades 2 through 5.

Potential Plexin Interaction Site

The Nrp-1/Plexin-A1 complex significantly differs in its binding properties for Sema3A from Nrp-1, suggesting that it presents a more extensive interaction surface containing a plexin component (Rohm et al., 2000; Takahashi et al., 1999). Many semaphorins from other classes (e.g., class 1, 2, 4, 7) directly bind plexins (Fiore and Püschel, 2003). A 70 amino acid region within the semaphorin domain (indicated with red in Figure 4E) harbors the signaling specificities of the molecules (Koppel et al., 1997). Since both Sema3A and Sema3D bind neuropilin-1 with high and comparable affinities (Feiner et al., 1997), the different biological activities of the two molecules are likely due to their utilization of different signaling coreceptors.

The Sema3A-65K structure reveals that residues 166–235 constitute the third β propeller blade. Interestingly, the largest semaphorin/semaphorin crystal-packing interface (dimerization is not considered crystal packing) maps to the same location, burying approximately 500 Å^2 of the side of the β propeller at blade 3 (Figure 4F). The total buried area in the two interacting molecules is approximately 1000 Å^2, which, although much smaller than the area buried in the semaphorin dimerization interface, is still significant, suggesting that the observed crystal-packing interface might represent a biologically

Figure 2. Sema3A-65K Forms Noncovalent Dimers in the Absence of Nrp-1 and Undergoes Dimer-to-Monomer Transition to Bind Nrp-1 with 1:1 Stoichiometry

(A) Two orthogonal stereoviews of the Sema3A-65K dimer in the asymmetric unit of the crystals. One of the monomers is in green, the other in blue.

(B–D) Sedimentation equilibrium studies of Sema3A-65K and Nrp-1 demonstrate that they associate to form 1:1 heterodimers. Shown are 30 μM samples of Sema3A-65K (B), Nrp-1AB (C), and Sema3A-65K/Nrp-1AB (D). The data fits best a single species with a molecular weight of 122 kDa for Sema3A-65K (the protein is a dimer), 64 kDa for Nrp-1AB, and 117 kDa for Sema3A-65K/Nrp-1AB.

(E) Sema3A-Δ1 and Sema3A-Δ2, unlike Sema3A-65K, are monomeric in solutions.

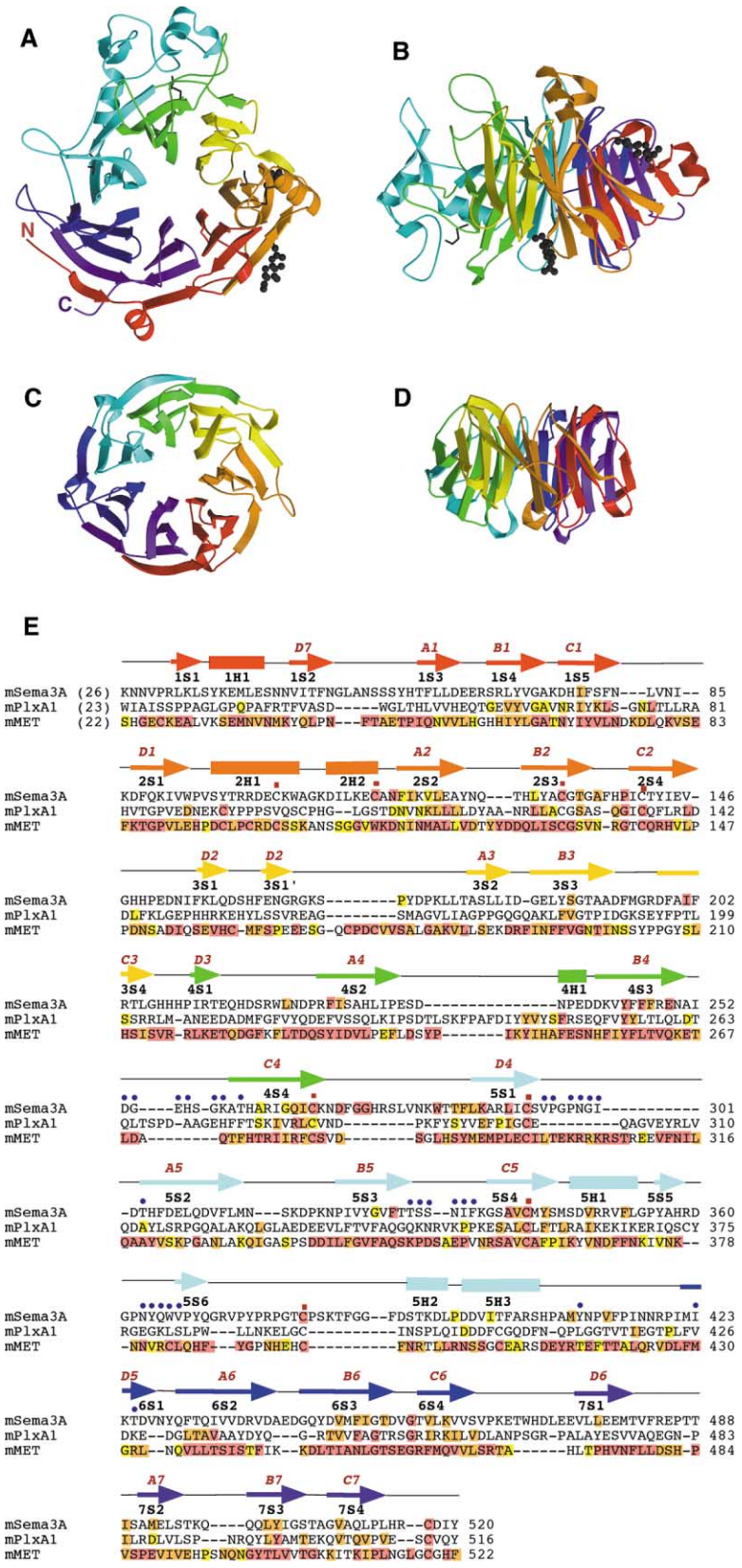

Figure 3. Structure of Sema3A-65K and Comparison with the Structure of the β Propeller of Transducin Gβ

(A) The structure of Sema3A-65K viewed from the "top" face of the molecule. The individual Sema3A-65K pseudorepeats are colored as in Figure 3E. The disulfide bonds and the N-acetyl-β-D-glucosamine moieties are colored in gray.

(B) A view along the side of the Sema3A-65K propeller.

(C and D) Corresponding views of the β propeller of the Gβ subunit of transducin (Sondek et al., 1996).

(E) Sequence alignment of the semaphorin domains of mouse semaphorin-3A, plexin-A1, and the MET receptor. The sequences were aligned using the program DNAstar. The secondary structure elements of the Sema3A crystal structure are shown using arrows for β strands and rectangles for α helices. The names of the Sema3A-65K secondary structure elements are listed below the secondary structure symbols. Alternative names corresponding to standard labeling practices for β propeller strands are given above the secondary structure symbols of β strands which have structural counterparts in the other known seven-bladed propeller structures. (The numbers in the "top" secondary-structure-element-labeling nomenclature identify the individual blades, while the numbers in the "bottom" nomenclature identify the individual sequence pseudorepeats.) The individual Sema3A-65K pseudorepeats corresponding to the individual propeller blades are colored (from N to C terminus) in red (1), orange (2), yellow (3), green (4), cyan (5), blue (6), and magenta (7). The color scheme is observed in all panels of the figure. The cysteines involved in disulfide bond formation are indicated with red squares above the sequences, and the residues that constitute the dimerization interface are indicated with blue circles. Conserved residues within each of the three receptor families (semaphorin, plexin, and Met) are indicated as follows: red, invariant; orange, highly conserved; yellow, moderately conserved.

relevant protein-protein interaction. Since the Sema3A/PlexinA1 interaction most probably involves a direct but weak binding between the semaphorin domains of the proteins, the semaphorin/semaphorin crystal-packing interface might mimic the ligand/coreceptor interface formed during signaling initiation.

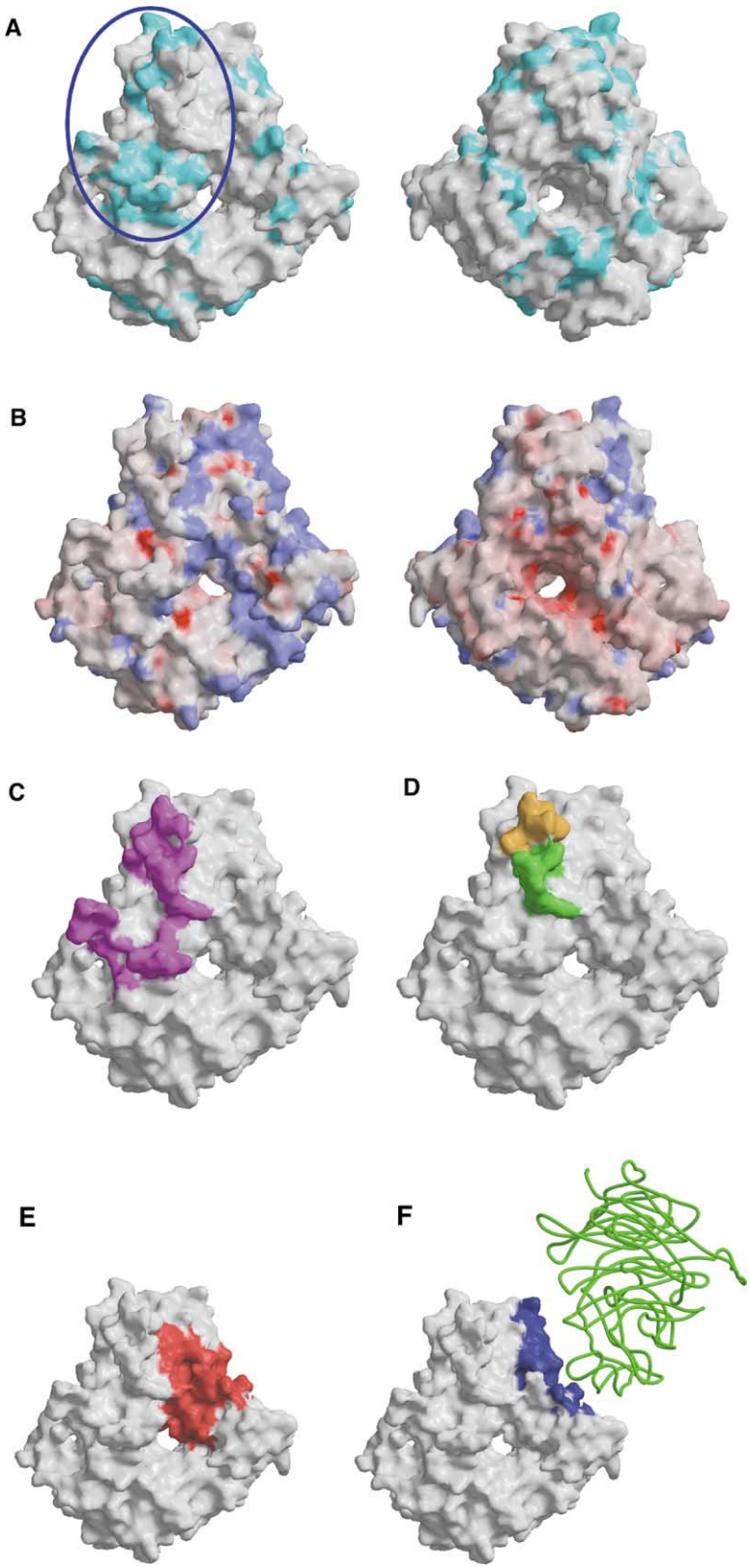

Figure 4. Molecular Surface of Sema3A-65K and Proposed Nrp-1 and Plexin Interaction Interfaces

(A) The residues, which are conserved within class 3 semaphorins (specifically in Sema3A, 3B, 3C, and 3F that have been shown to interact with neuropilins) but not conserved between class 3 and class 4 semaphorins (the latter do not bind neuropilins), are colored in cyan. The "top" face of the molecule is on the left, and the "bottom" face is on the right.

(B) Electostatic surface potential of Sema3A-65K. Red and blue represent electrostatic potentials in the range of −11 to +11 k_BT, where k_B is the Boltzman constant and T is the temperature (293 K). The "top" face of the molecule is on the left, and the "bottom" face is on the right.

(C) The Sema3A-65K dimerization interface at the "top" face of the molecule is colored in magenta (total buried is 2900 A^2).

(D) Structure-based mutagenesis identifies Nrp-1-interacting residues. The surface loop deleted in Sema3A-Δ1 is in green, and the loop deleted in Sema3A-Δ2 is in orange. The latter is also the target of a semaphorin3A-neutralizing antibody, and peptides derived from this region (residues 363−380) induce Sema3A-specific biological responces (Shirvan et al., 2002).

(E) Residues suggested to determine coreceptor preferences are shown in red. The highlighted region corresponds to the specificity-conferring stretch (residues 166−235) identified in sequence-swapping experiments between SemaA and Sema3D (Koppel et al., 1997).

(F) The Sema3A-65K crystal-packing interface at the side of the β propeller is colored in blue (total buried is 1000 A^2). The Cα trace of the interacting Sema3A-65K molecule is in green.

Plexin Autoinhibition

The presence and the specific localization of the ligand binding β propeller domains in plexins and the LDL receptor (LDLR) suggests that they might share a similar autoinhibition mechanism (Figure 5B) (Rudenko et al., 2002; Takahashi and Strittmatter, 2001). In both cases,

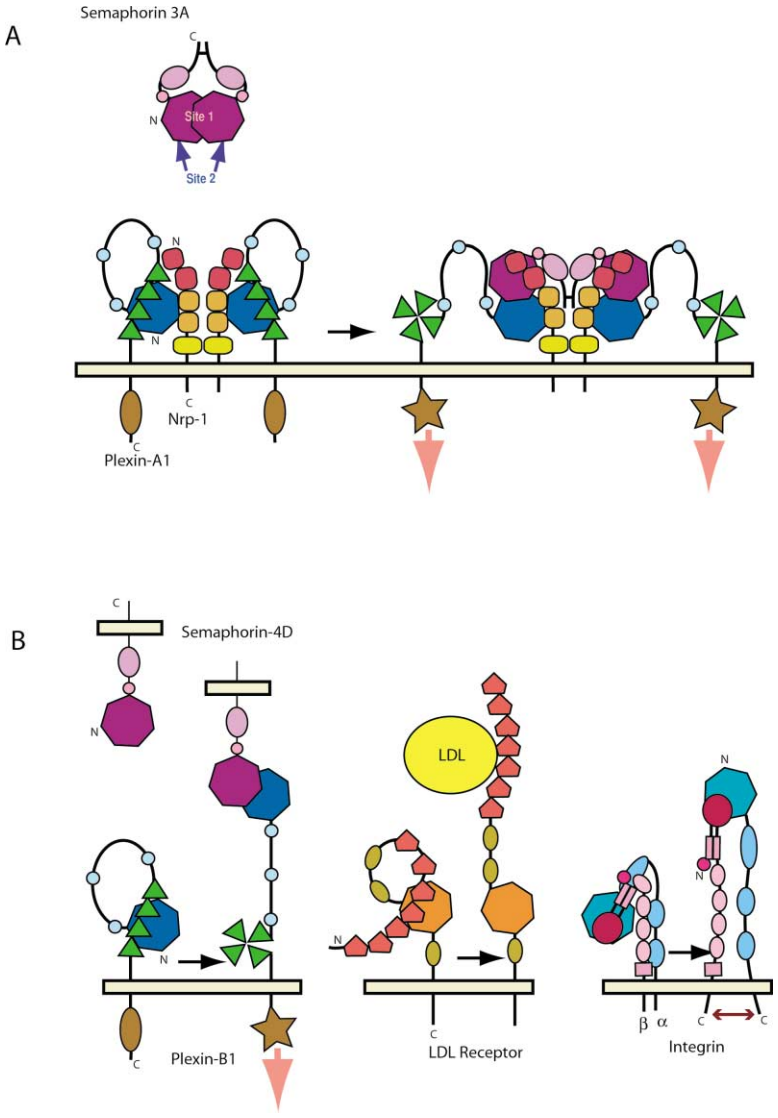

Figure 5. Model for Semaphorin Signaling

(A) Initiation of Sema3A-mediated signaling via the Nrp-1/Plexin-A1 complex (see discussion in text). Sema3A is in magenta (Sema domain, heptagon; PSI domain, circle; Ig domain, oval). In plexin, the Sema domain is in dark blue, the IPT domains in green, and the PSI regions in light blue. The intracellular SexPlexin domain is in brown, and the star corresponds to the activated form (the red arrow indicates signaling directing growth cone collapse). In Nrp-1, the A1 and A2 domains are in red, B1 and B2 are in orange, and the MAM domain is in yellow. Sema3A binding results in a 2:2:2 ligand/receptor/coreceptor complex formation and the release of the plexin membrane-proximal extracellular region, which in the absence of constrains adopts an active conformation (right panel).

(B) (Left panel) Initiation of Sema4D signaling via the Plexin-B1 receptor. In this case, no coreceptors are required. As with Sema3A, ligand binding disrupts the inhibitory semaphorin conformation, resulting in activation of downstream signaling. (Middle panel) The LDL receptor and plexins share a structurally similar autoinhibition mechanism. In both cases, the β propeller domains (heptagons) function as an alternate substrate and bind in *cis* other domains of the receptors, thus inhibiting the molecules. The inhibition of the LDLR is relieved at high pH, allowing the β propeller domain to be displaced by LDL. (Right panel) Integrin activation. The α subunit is in blue, and the β is in red. The large conformational change in plexins that accompanies the release of autoinhibition is reminiscent of the rearrangement of integrin ectodomains during activation. Interestingly, integrins have also been shown to undergo an intracellular domain separation (brown arrow) concomitant with receptor activation (Kim et al., 2003). In addition, plexins and integrins may share inside-out signaling.

the β propeller domain functions as an alternate substrate and binds in *cis* other receptor domains (the LA4/R4 and LA5/R5 cysteine-rich modules in LDLR and the IPT domains of plexins), thus inhibiting the molecules. The inhibition of the LDLR is relieved at high pH, allowing the β propeller domain to be displaced by LDL. In plexins, on the other hand, interactions with the semaphorin domain of their ligands presumably dissociates the inhibitory complex, resulting in activation of downstream signaling. Interestingly, the LA4/LA5 binding site on the LDL β propeller domain is centered on blades 4 and 5 at the "top" face of the molecule, occupying the same general location as the proposed neuropilin-interaction site on the Sema3A semaphorin domain.

A Model for Initiation of Semaphorin Signaling

Our results, in conjunction with previously published data (Giger et al., 1998; Gu et al., 2002; Nakamura et al., 1998; Renzi et al., 1999; Takahashi and Strittmatter, 2001; Tamagnone et al., 1999), suggest that the following molecular events occur during the initiation of semaphorin signaling (Figure 5). In the absence of ligand, plexins assume an autoinhibited state where their N-terminal semaphorin domain intramolecularly interacts with the C-terminal part (IPT sequences) of the ectodomain, constraining the juxtamembrane and intercellular domains in an inactive conformation. Nrp-1 interacts with both the semaphorin domain and the IPT region of Plexin-A1 (Takahashi and Strittmatter, 2001) and thus stabilizes the autoinhibited conformation of the molecule. Binding of Sema3A to Nrp-1 leads to a conformational change in Plexin-A1 that is transmitted to the cytosolic domain. We suggest that Sema3A contains two distinct interaction surfaces. One is more extensive, overlaps with the Sema3A-65K dimerization interface (Figure 5A, site 1), and is responsible for the initial high-affinity binding to the AB domain of Nrp-1. The second site (Figure 5A, site 2) is smaller and located at the side of the β propeller. The binding of Sema3A to Nrp-1 presents site 2 for binding to the Plexin-A1 semaphorin domain. The ensuing Sema3A/plexinA1 interaction displaces the bound IPT region and releases the plexin

juxtamembrane and intercellular domains from their inactive conformation, initiating downstream signaling. In the activated receptor, Nrp-1 remains associated with Plexin-A1 through a direct interaction with its semaphorin domain. The interaction with the C-terminal half of the Plexin-A1 ectodomain may also be preserved (Takahashi and Strittmatter, 2001). The two coreceptors interact also indirectly, through the bound Sema3A ligand. Some plexins, such as Plexin-B1 are directly activated by semaphorins (Tamagnone et al., 1999). In this case, the interaction between the semaphorin domains of the ligand and receptor is of high affinity, and the binding does not require assistance from a neuropilin (Figure 5B, left panel).

Finally, the large conformational change in plexins that likely accompanies the release of autoinhibition is reminiscent of the rearrangement of integrin ectodomains after their activation (Figure 5B, right panel). Interestingly, the interaction of Rac with the cytoplasmic domain of Plexin-B1 leads to an increase in its affinity for Sema4D and its transport to the plasma membrane (Vikis et al., 2002), suggesting a similar mechanism of inside-out signaling that is used by integrins (Hynes, 2002; Takagi et al., 2002). Furthermore, plexins and integrins may both utilize a novel activation mechanism (Figure 5) where their intracellular signaling domains are held in close proximity to each other in the inactive state and undergo significant spatial separation upon receptor activation (Kim et al., 2003; Takahashi and Strittmatter, 2001).

Experimental Procedures

Protein Expression and Purification

Mouse Sema3A-65K (residues 26–546) was cloned in the pAcGP67B baculovirus vector with a 6xHis-tag at the N terminus. Mouse Nrp-1AB (residues 27–583), Nrp-1A (residues 27–265), and Nrp-1B (residues 274–583) were cloned in the pVL-VSV baculovirus vector with a 6xHis-tag at the N terminus. The recombinant baculovirus vectors were cotransfected with BaculoGold DNA (PharMingen) in SF9 cells. Passage 4 was used to infect Hi5 cells in suspension at a density of 1.8×10^6 cells/ml in EX-CELL-405 serum-free media (JRH Biosciences). Infected cells were grown at 27°C and 110 rpm and harvested after 64 hr. For the production of Selenomethionine (SeMet) Sema3A, 22 hr after the infection the cells were spun down and the media was changed to EX-CELL-405 Modified (methionine deficient). The cells were grown for additional 3.5 hr ("starvation" period) to lower the intracellular pool of methionine, spun down, and the media was changed to methionine deficient supplemented with 120 mg/l SeMet. The cells were harvested 64 hr after infection. The proteins were purified using cobalt-chelating and gel-filtration chromatography.

Mutagenesis

Sema3A receptor binding mutants (Sema3A-Δ1 lacks residues 252–260 and has Ala 251 substituted with a glycine; Sema3A-Δ2 lacks residues 359–366 and has His 358 and Val 367 substituted with glycines; the glycines were introduced to allow mainchain flexibility) were generated using QuickChange Mutagenesis Kit (Stratagene) and confirmed by automatic DNA sequencing. Sema3A-Δ1 and Sema3A-Δ2 were indistinguishable from Sema3A-65K as judged by CD spectroscopy and behaved in identical fashion during purification, with the exception of being monomeric rather than dimeric on gel filtration (data not shown).

Fluorescence Titration

Measurements were done on a FluoroMax-2 spectrofluorimeter (SPEX) in a time drive mode using 10 mm pathlength fluorescence cuvettes. The excitation and emission wavelengths were 295 and 350 nm (respectively), and slit widths were 5 nm. The temperature was kept at a constant 25°C. Titrations were done by adding small volumes of concentrated (0.5 mM) Sema3A-65K (or Sema3A-Δ1 or Sema3A-Δ2) solution to a cuvette containing 2 ml of a 0.5 μM solution of Nrp-1A, Nrp-1B, or Nrp-1AB in 10 HEPES buffer (pH 7.5) and allowing the mixture to equilibrate for 5 min. The volume of added Sema3A never exceeded 5% of the total volume. A difference between the fluorescence units (Δ F.U.) of the complex in comparison to the theoretical value, calculated from the individual fluorescence units of Nrp-1 and Sema3A (with "KaleidaGraph" software), was used to calculate the binding affinity.

Analytical Ultracentrifugation

Measurements were performed on a Beckman XL-A centrifuge equipped with an An-60 Ti rotor. Protein solutions were loaded at initial concentrations of 30, 3, and 1 μM in 10 mM HEPES (pH 7.5), 0.4 M KCl, and analyzed at rotor speeds of 8 and 11 krpm for Sema3A-65K and Sema3A-65K/Nrp-1AB, and 13 and 16 krpm for Nrp-1AB, Sema3A-Δ1, and Sema3A-Δ2 at 20°C. Data were acquired at two wavelengths per rotor speed and processed simultaneously with a nonlinear least squares fitting routine.

Collapse Assay

The COS-7 collapse assay was done as described previously (Zanata et al., 2002) and the number of collapsed cells determined (n = 3 coverslips per value; approximately 300 to 500 cells were counted per coverslip).

Crystallization and Structure Determination

Purified Sema3A-65K was concentrated to 15 mg/ml and crystallized in a hanging drop at 20°C against a reservoir containing 100 mM Tris Hydrochloride (pH 8.5), 30 mM Heptyl-β-D-thioglucoside, and 8% Polyethylene Glycol 8,000. The space group is C2 with a = 219.38 Å, b = 59.83 Å, c = 122.91 Å, β = 109.0, and two molecules in the asymmetric unit. Data were collected at beamlines NE-CAT (APS) and F2 (CHESS). All data were processed using DENZO and SCALEPACK (Otwinowski and Minor, 1997). The locations of the Se atoms were identified with the program SnB (Miller et al., 1993). The peaks were refined using MLPHARE (CCP4, 1994). Model building proceeded through an iterative process of building in O and refinement of the model in CNS (Jones et al., 1991; Brünger et al., 1998).

Acknowledgments

This work was upported by the New York State Spinal Cord Injury Research Program (D.B.N) and by DFG and Fonds der Chemischen Industrie (A.W.P.). D.B.N. is a Bressler Scholar. We thank Dr. Craig Ogata for assistance with crystallographic data collection.

Received: June 19, 2003
Revised: July 17, 2003
Accepted: July 30, 2003
Published: August 13, 2003

References

Adams, R.H., Lohrum, M., Klostermann, A., Betz, H., and Püschel, A.W. (1997). The chemorepulsive activity of secreted semaphorins is regulated by furin-dependent proteolytic processing. EMBO J. *16*, 6077–6086.

Bork, P., Doerks, T., Springer, T.A., and Snel, B. (1999). Domains in plexins: links to integrins and transcription factors. Trends Biochem. Sci. *24*, 261–263.

Brünger, A.T., Adams, P.D., Clore, G.M., DeLano, W.L., Gros, P., Grosse-Kunstleve, R.W., Jiang, J.S., Kuszewski, J., Nilges, M., Pannu, N.S., et al. (1998). Crystallography and NMR system: A new software suite for macromolecular structure determination. Acta Crystallogr. D Biol. Crystallogr. *54*, 905–921.

Collaborative Computational Project. (1994). The CCP4 suite: programs for X-ray crystallography. Acta Crystallogr. D Biol. Crystallogr. *50*, 760–763.

Feiner, L., Koppel, A.M., Kobayashi, H., and Raper, J.A. (1997). Secreted chick semaphorins bind recombinant neuropilin with similar affinities but bind different subsets of neurons in situ. Neuron *19*, 539–545.

Fiore, R., and Püschel, A.W. (2003). The function of semaphorins during nervous system development. Front. Biosci. *8*, S484–S499.

Fulop, V., and Jones, D.T. (1999). Beta propellers: structural rigidity and functional diversity. Curr. Opin. Struct. Biol. *9*, 715–721.

Giger, R.J., Urquhart, E.R., Gillespie, S.K., Levengood, D.V., Ginty, D.D., and Kolodkin, A.L. (1998). Neuropilin-2 is a receptor for semaphorin IV: insight into the structural basis of receptor function and specificity. Neuron *21*, 1079–1092.

Gu, C., Limberg, B.J., Whitaker, G.B., Perman, B., Leahy, D.J., Rosenbaum, J.S., Ginty, D.D., and Kolodkin, A.L. (2002). Characterization of neuropilin-1 structural features that confer binding to semaphorin 3A and vascular endothelial growth factor 165. J. Biol. Chem. *277*, 18069–18076.

He, Z., and Tessier-Lavigne, M. (1997). Neuropilin is a receptor for the axonal chemorepellent Semaphorin III. Cell *90*, 739–751.

Holm, L., and Sander, C. (1998). Touring protein fold space with Dali/FSSP. Nucleic Acids Res. *26*, 316–319.

Hynes, R.O. (2002). Integrins: bidirectional, allosteric signaling machines. Cell *110*, 673–687.

Jones, T.A., Zou, J.Y., Cowan, S.W., and Kjeldgaard, M. (1991). Improved methods for building protein models in electron density maps and the location of errors in these models. Acta Crystallogr. A *47*, 110–119.

Kim, M., Carman, C.V., and Springer, T.A. (2003). Bidirectional transmembrane signaling by cytoplasmic domain separation in integrins. Science, in press.

Klostermann, A., Lohrum, M., Adams, R.H., and Püschel, A.W. (1998). The chemorepulsive activity of the axonal guidance signal semaphorin D requires dimerization. J. Biol. Chem. *273*, 7326–7331.

Kolodkin, A.L., Levengood, D.V., Rowe, E.G., Tai, Y.T., Giger, R.J., and Ginty, D.D. (1997). Neuropilin is a semaphorin III receptor. Cell *90*, 753–762.

Koppel, A.M., and Raper, J.A. (1998). Collapsin-1 covalently dimerizes, and dimerization is necessary for collapsing activity. J. Biol. Chem. *273*, 15708–15713.

Koppel, A.M., Feiner, L., Kobayashi, H., and Raper, J.A. (1997). A 70 amino acid region within the semaphorin domain activates specific cellular response of semaphorin family members. Neuron *19*, 531–537.

Lee, C.C., Kreusch, A., McMullan, D., Ng, K., and Spraggon, G. (2003). Crystal structure of the human neuropilin-1 b1 domain. Structure *11*, 99–108.

Miller, R., DeTitta, G.T., Jones, R., Langs, D.A., Weeks, C.M., and Hauptman, H.A. (1993). On the application of the minimal principle to solve unknown structures. Science *25*, 1430–1433.

Nakamura, F., Tanaka, M., Takahashi, T., Kalb, R.G., and Strittmatter, S.M. (1998). Neuropilin-1 extracellular domains mediate semaphorin D/III-induced growth cone collapse. Neuron *21*, 1093–1100.

Otwinowski, Z., and Minor, W. (1997). Processing of X-ray diffraction data collected in oscillation mode. In Methods in Enzymology, Volume 276: Macromolecular Crystallography, part A, C.W. Carter, Jr, and R.M. Sweet, eds. (New York: Academic Press), pp. 307–326

Paoli, M. (2001). Protein folds propelled by diversity. Prog. Biophys. Mole. Biol. *76*, 103–130.

Renzi, M.J., Feiner, L., Koppel, A.M., and Raper, J.A. (1999). A dominant negative receptor for specific secreted semaphorins is generated by deleting an extracellular domain from neuropilin-1. J. Neurosci. *19*, 7870–7880.

Robinson, R.C., Turbedsky, K., Kaiser, D.A., Marchand, J.B., Higgs, H.N., Choe, S., and Pollard, T.D. (2001). Crystal structure of Arp2/3 complex. Science *294*, 1679–1684.

Rohm, B., Ottemeyer, A., Lohrum, M., and Püschel, A.W. (2000). Plexin/neuropilin complexes mediate repulsion by the axonal guidance signal semaphorin 3A. Mech. Dev. *93*, 95–104.

Rudenko, G., Henry, L., Henderson, K., Ichtchenko, K., Brown, M.S., Goldstein, J.L., and Deisenhofer, J. (2002). Structure of the LDL receptor extracellular domain at endosomal pH. Science *298*, 2353–2358.

Shirvan, A., Kimron, M., Holdengreber, V., Ziv, I., Ben-Shaul, Y., Melamed, S., Melamed, E., Barzilai, A., and Solomon, A.S. (2002). Anti-semaphorin 3A antibodies rescue retinal ganglion cells from cell death following optic nerve axotomy. J. Biol. Chem. *277*, 49799–49807.

Sondek, J., Bohm, A., Lambright, D.G., Hamm, H.E., and Sigler, P.B. (1996). Crystal structure of a G-protein beta gamma dimer at 2.1A resolution. Nature *397*, 369–374.

Sprague, E.R., Redd, M.J., Johnson, A.D., and Wolberger, C. (2000). Structure of the C-terminal domain of Tup1, a corepressor of transcription in yeast. EMBO J. *19*, 3016–3027.

Takagi, J., Petre, B.M., Walz, T., and Springer, T.A. (2002). Global conformational rearrangements in integrin extracellular domains in outside-in and inside-out signaling. Cell *110*, 599–611.

Takahashi, T., and Strittmatter, S.M. (2001). PlexinA1 autoinhibition by the plexin sema domain. Neuron *29*, 429–439.

Takahashi, T., Fournier, A., Nakamura, F., Wang, L.H., Murakami, Y., Kalb, R.G., Fujisawa, H., and Strittmatter, S.M. (1999). Plexin-neuropilin-1 complexes form functional semaphorin-3A receptors. Cell *99*, 59–69.

Tamagnone, L., Artigiani, S., Chen, H., He, Z., Ming, G.I., Song, H., Chedotal, A., Winberg, M.L., Goodman, C.S., Poo, M., et al. (1999). Plexins are a large family of receptors for transmembrane, secreted, and GPI-anchored semaphorins in vertebrates. Cell *99*, 71–80.

Varghese, J.N., Laver, W.G., and Colman, P.M. (1983). Structure of the influenza virus glycoprotein antigen neuraminidase at 2.9 A resolution. Nature *303*, 35–40.

Vikis, H.G., Li, W., and Guan, K.L. (2002). The plexin-B1/Rac interaction inhibits PAK activation and enhances Sema4D ligand binding. Genes Dev. *16*, 836–845.

Xiong, J.P., Stehle, T., Diefenbach, B., Zhang, R., Dunker, R., Scott, D.L., Joachimiak, A., Goodman, S.L., and Arnaout, M.A. (2001). Crystal structure of the extracellular segment of integrin alpha Vbeta3. Science *294*, 339–345.

Zanata, S.M., Hovatta, I., Rohm, B., and Püschel, A.W. (2002). Antagonistic effects of Rnd1 and RhoD GTPases regulate receptor activity in Semaphorin 3A-induced cytoskeletal collapse. J. Neurosci. *22*, 471–477.

Accession Numbers

Coordinates for the Sema3A-65K structure have been deposited in the Protein Data Bank (1Q47).